

## Antiferromagnetic order in a Dy/Er superlattice

K. Dumesnil, C. Dufour, M. Vergnat, G. Marchal, and Ph. Mangin

*Laboratoire de Métallurgie Physique et Sciences des Matériaux, Université de Nancy I, 54506 Vandoeuvre Cedex, France*

M. Hennion

*Laboratoire Léon Brillouin, Centre d'Etudes de Saclay, 91191 Gif-sur-Yvette Cedex, France*

W. T. Lee, H. Kaiser, and J. J. Rhyne

*University of Missouri, Columbia, Missouri 65211*

(Received 15 November 1993)

We present results on magnetic ordering in a Dy(60 Å)/Er(60 Å) superlattice made up of two magnetic rare earths exhibiting in-plane and perpendicular anisotropies. Neutron diffraction reveals that the helical magnetic coherence of dysprosium propagates through paramagnetic erbium layers, without inducing spin ordering in erbium. Below the ordering temperature of dysprosium individual ferromagnetic dysprosium layers show antiparallel stacking through magnetic erbium. This antiferromagnetic phase of dysprosium is irreversibly destroyed by a 5.5-kOe external magnetic field and replaced by a ferromagnetic order between dysprosium layers. Magnetization measurements indicate that this irreversibility could arise from an energy barrier between parallel and antiparallel stacking of ferromagnetic dysprosium layers.

Rare-earth superlattices have recently provided new insight into magnetism, in particular the coherent propagation of helical order through nonmagnetic layers and the effects of epitaxial strain on magnetic transition temperatures. The propagation of helical order was first shown in the Dy/Y system<sup>1</sup> and was observed later in Er/Y (Ref. 2) and in Dy/Lu (Ref. 3) superlattices. Its origin was shown to lie in the  $q$  dependence of the generalized susceptibility of yttrium and of lutetium<sup>4</sup> that has maxima at  $q$  values different from zero, and by the stabilization of the spin-density wave in these materials. The second effect due to epitaxy concerns the lowering (or enhancing) of the ferromagnetic transition temperature ( $T_c$ ) from effects of internal strain clamping of the magnetostrictive modes that drive in the transition. In Dy/Y superlattices, the negative mismatch ( $-1.6\%$ ) between dysprosium and yttrium expands the basal plane of dysprosium and leads to the suppression of the ferromagnetic transition. Conversely in Dy/Lu superlattices, the  $+2.4\%$  mismatch leads to an epitaxial compression of the dysprosium basal plane which enhances the Curie temperature (the temperature at which the magnetic moments orientate parallelly in each layer) by nearly 100%. Recently an antiferromagnetic interlayer coupling was observed in Dy/Lu superlattices.<sup>3</sup> The authors showed that the ferromagnetic dysprosium layers were stacked antiparallel and explained this effect by a local dipolar coupling. They showed that the superlattice undergoes a cooperative magnetic distortion, breaking into approximate 300-Å orthorhombic domains oriented along three equivalent easy axes, which allow for dipolar coupling between successive dysprosium layers through the nonmagnetic lutetium layers.

In this paper we report our observation of the propaga-

tion of the helical order of dysprosium spins through the paramagnetic phase of a strong magnetic element. Then we show that at low temperature there is a long-range antiferromagnetic interlayer coupling between ferromagnetic sheets of dysprosium spins through magnetically ordered erbium layers. The antiferromagnetic interlayer stacking can be destroyed by application of an external magnetic field and replaced by a ferromagnetic ordering between dysprosium layers. The antiferromagnetic arrangement does not reappear at low temperatures after switching off the field, but it is necessary to recycle the sample up to the ferromagnetic transition of dysprosium to restore the antiferromagnetic order.

In bulk form hcp dysprosium is known to exhibit a strong basal-plane anisotropy. It orders magnetically in a basal-plane spiral at 179 K that transforms at 85 K into a ferromagnetic state with the magnetization direction along the easy- $a$  axis. This transition is driven by a reduction in the magnetoelastic energy associated with the ferromagnetic state compared to the helical one.<sup>5</sup> The magnetic structure of erbium favors a  $c$ -axis spin direction and is more complex than that of dysprosium.<sup>6</sup> At 84 K, erbium orders into a modulated moment configuration in which the  $c$ -axis component of the magnetization has a sine wave amplitude modulation with a period of approximately seven atomic layers and the transverse moment components are disordered. Below 52 K, the  $c$ -axis component is square-wave modulated and the basal-plane component exhibits helical order. In this temperature range, erbium exhibits a discrete sequence of intermediate commensurate spin states. At 19 K the  $c$ -axis component orders ferromagnetically, resulting in a conical moment state persisting to low temperature. The mismatch between dysprosium and erbium is  $+0.9\%$ ,

and therefore tends to compress slightly the dysprosium basal plane favoring the ferromagnetic alignment of dysprosium spins.

The present superlattice samples were grown by molecular-beam epitaxy using the method proposed by Kwo, Hong, and Nakahara.<sup>7</sup> The base pressure was  $2 \times 10^{-11}$  Torr. A 1000-Å-thick (110) bcc niobium buffer was first grown on a (11 $\bar{2}$ 0) sapphire substrate to avoid oxidation of the rare earths. A (0001) 500-Å-thick yttrium layer was then grown on the niobium buffer to relieve interface strains. During the (0001) Dy/Er superlattice deposition, the temperature was held at 350 °C to minimize interdiffusion and the pressure was maintained in the  $10^{-9}$ -Torr range. The deposition rates were regulated at 0.5 Å/s using a very sensitive optical sensor. The number of deposited Dy/Er bilayers was 60. The sample was finally covered by a 500-Å-thick yttrium layer. Room-temperature x-ray diffraction showed good crystal quality with mosaic width of about 0.3°. Based on the narrow width of the Bragg peak and the positions of the satellite harmonics (three on each side), the superlattice has a coherence length over 700 Å and its periodicity is 120 Å.

Neutron-scattering experiments were performed at the Laboratoire Léon Brillouin in Saclay (LLB) and at the Missouri University Research Reactor in Columbia on triple-axis spectrometers. The data presented in Fig. 1 were obtained on the G43 Instrument of the LLB with an incident wavelength of 4.245 Å and a collimation of 30" on each side of the sample. A field up to 5.5 kOe was applied in the plane of the sample, which is the easy magnetic plane for dysprosium and the hard magnetic plane for erbium.

The three neutron-scattering diffraction patterns in Fig. 1 were collected from a Dy(60 Å)/Er(60 Å) sample (a) at 110 K in zero field (b) at 12 K in zero field, and (c) at 12 K under a 5.5-kOe external magnetic field. At 110 K, the diffraction pattern exhibits a principal (002) Bragg peak from the superlattice at  $q = 2.240 \text{ \AA}^{-1}$  corresponding to a parameter  $c = 5.61 \text{ \AA}$  that is the weighted average of pure dysprosium and erbium parameters. A structural modulation satellite of the main peak is superposed on the (002) Bragg peak of yttrium at  $q = 2.188 \text{ \AA}^{-1}$ . On each side, we observe a set of magnetic satellites (absent in the data taken at 200 K) that are typical of helical structures coherent over large distances. These results show that dysprosium exhibits a basal-plane helical order and that the magnetization wave is coherent through erbium layers that are themselves paramagnetic as shown by the absence of magnetic satellites about the (10 $\bar{1}$ 0) reflection. Thus, the magnetic dysprosium and erbium layers act independently and there is no tendency for the superlattice to undergo uniform three dimensional magnetic order. From the full width at half maximum of the left side magnetic satellite, the coherence length of the dysprosium helix is calculated to be about 350 Å. The neutron-diffraction data have been analyzed by least-squares fitting to a structure factor containing both nuclear and magnetic components. The best adjustment is obtained with a  $5\mu_B$  atomic magnetic moment and a turn angle of 30° for the dysprosium, and a turn angle of 46° for erbium. This value is close to the turn angle of

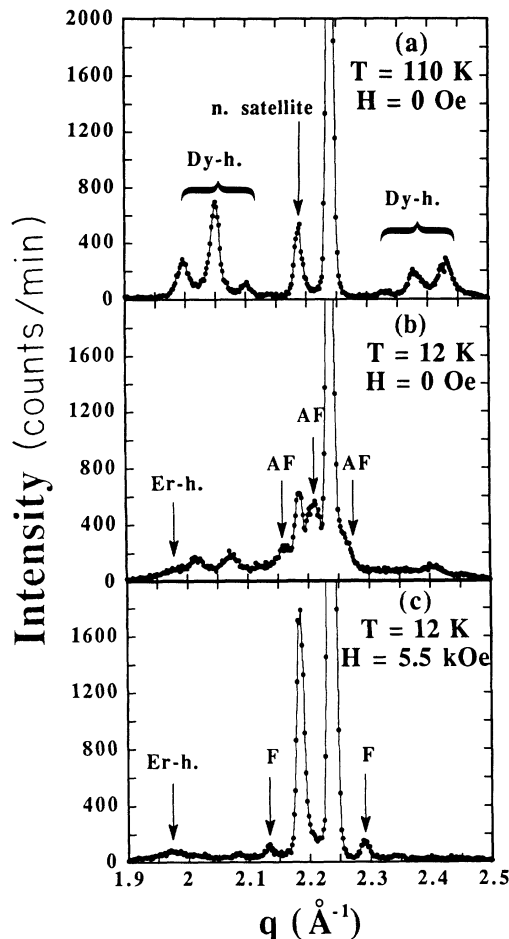


FIG. 1. Neutron-diffraction patterns along the (0001) direction for a Dy (60 Å)/Er(60 Å) superlattice: (a) at 110 K under zero-field. The main peak (at  $q = 2.24 \text{ \AA}^{-1}$ ) intensity reaches 4000 cts/min. A nuclear modulation satellite (*n. satellite*) is at  $q = 2.188 \text{ \AA}^{-1}$ . The helix of dysprosium gives rise to magnetic peaks indicated by braces (Dy-h.). (b) At 12 K under zero-field. The intensity of the main Bragg peak is unchanged but new antiferromagnetic peaks (AF) have emerged. A magnetic satellite due to the helix of erbium (Er-h.) is observed near  $1.975 \text{ \AA}^{-1}$ . (c) At 12 K under a 5.5-kOe magnetic field applied in the basal plane. The main peak intensity reaches 7000 cts/min. The antiferromagnetic peaks have disappeared. A ferromagnetic contribution (F) adds to the superlattice satellites.

the conical phase of ordered erbium. Even though erbium is paramagnetic, an "effective turn angle" can be assigned to the erbium spin-density wave that is induced by the dysprosium ordering. The existence of a spin-density-wave-like coupling is manifested by the phase coherence of the helical order extending over several bilayers. This phase coherence is the first demonstration of the propagation of a spin-density wave through a magnetic rare earth that is remaining in a paramagnetic state.

At 12 K under zero field [Fig. 1(b)] some residual magnetic satellite peaks are still present, broader and far less intense, and whose positions correspond to a turn angle of about 27°. The intensities of the main Bragg peak ( $q = 2.238 \text{ \AA}^{-1}$ ) and of the superlattice satellite located at  $q = 2.185 \text{ \AA}^{-1}$  are unchanged, but a new peak has

emerged between these two peaks at  $q = 2.21 \text{ \AA}^{-1}$ . This peak corresponds to a double periodicity of the superlattice and is attributed, as in Dy/Lu superlattices, to an antiferromagnetic stacking of ferromagnetic dysprosium layers. This is confirmed by the presence of a second antiferromagnetic peak to the left side of the main peak at  $q = 2.162 \text{ \AA}^{-1}$  and of a small one at  $q = 2.257 \text{ \AA}^{-1}$ . The width of these new antiferromagnetic peaks is larger than that of the main peak and its superlattice satellite. The in-plane ordering of the conical structure of erbium is shown by the satellite near  $q = 1.975 \text{ \AA}^{-1}$ . It corresponds to a turn angle of  $41^\circ$  in erbium layers which is approximately that of bulk erbium.

Spectrum 1(c) has been collected at 12 K under a 5.5-kOe magnetic field applied in the basal plane. We observe first that the magnetic satellites of the dysprosium helix have disappeared. The remaining broad satellite is due to the conical phase of erbium that is not destroyed by this in-plane magnetic field. The 5.5-kOe magnetic field applied in the basal plane is too weak to turn the erbium magnetization from the  $c$ -axis direction. The second consequence of the applied field is the disappearance of the antiferromagnetic peak, accompanied by an increase of the intensities of the main peak at  $q = 2.237 \text{ \AA}^{-1}$  and of its superlattice satellite at  $q = 2.185 \text{ \AA}^{-1}$ , and by the appearance of two new satellites whose positions ( $q = 2.134 \text{ \AA}^{-1}$  and  $q = 2.340 \text{ \AA}^{-1}$ ) are expected from the superlattice modulation. This clearly indicates that the dysprosium moments are now coupled parallel from layer to layer.

After removing the magnetic field, the diffraction pattern of Fig. 1(b) is not recovered but remains exactly that of Fig. 1(c). The dysprosium layers retain ferromagnetic alignment and neither the antiferromagnetic peak nor the residual magnetic peaks of the dysprosium helix reappear. It is necessary to warm the system to about 80 K, and subsequently cool it down under zero field, to observe the diffraction pattern of Fig. 1(b) again. If the sample is cooled in the applied field, the diffraction pattern of Fig. 1(c) is observed.

The irreversibilities observed at low temperature by neutron-scattering experiments were investigated by magnetization measurements performed using a standard superconducting quantum interference device magnetometer. The sample was cooled to 12 K under zero-field and the first magnetization curve and the hysteresis cycle were determined with the magnetic field applied along the  $a$  axis (Fig. 2). The magnetization increases slowly in the 0–1 kOe range and more rapidly from 1 to 3 kOe with a change in curvature. After saturation of the magnetization, the hysteresis loop exhibits vertical lines at the coercive fields  $\pm 1.6$  kOe. This reveals that the system remains clearly ferromagnetic with a sudden cooperative change of the magnetization direction at  $H_c$  without any other intermediate spin state. The high value of  $H_c$  is to be compared with a smaller value (500 Oe) observed for a 4500-Å-thick single layer of dysprosium grown on yttrium. In a single layer the magnetization reversal results from domain-wall displacements, whereas in multilayers the effect is more cooperative, perhaps closer to that observed in fine particle systems. The shape of the initial

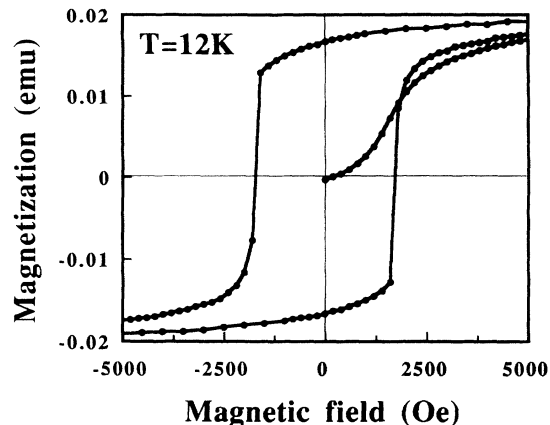


FIG. 2. Hysteresis loop at 12 K with the magnetic field applied in the plane of the sample for a Dy (60 Å)/Er (60 Å) superlattice.

magnetization curve, obtained after zero-field cooling, is clearly due to the rotation toward the field direction of the magnetic moments which were antiparallel to the field. When the field is switched off, the antiparallel ordering is not recovered because the antiferromagnetic coupling is by far too weak for spins to cross the energy barrier. The magnetizations of all layers turn simultaneously as in single domains at  $H_c$  when the field is reversed. We observed that the shape of the hysteresis loop obtained from the same sample with magnetic field ap-

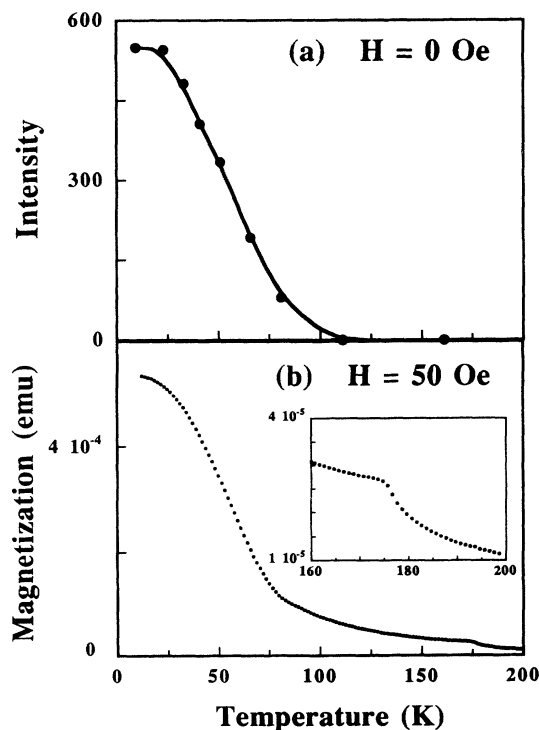


FIG. 3. (a) Intensity of the antiferromagnetic peak ( $q = 2.21 \text{ \AA}^{-1}$ ) versus temperature under zero-field. (b) Field-cooled magnetization versus temperature under a 50-Oe in-plane applied magnetic field for a Dy(60 Å)/Er(60 Å) superlattice.

plied along the  $b$  direction is not significantly different. Magnetization measurements performed with the magnetic field applied along the  $c$  axis are typical of erbium and show that the magnetization of this element is oriented perpendicular to the plane of the sample.

In order to explore the thermal dependence of the antiferromagnetic order, we followed the variation of the intensity of the antiferromagnetic peak measured by neutron scattering under zero field. As shown in Fig. 3(a), it appears at about 80 K, close both to the ferromagnetic transition of bulk dysprosium and to the Néel temperature of bulk erbium. The appearance of the antiferromagnetic peak coincides approximately to the increase of the magnetization observed during a low-field cooling of the sample [Fig. 3(b)]. The magnetization curve obtained under a 50-Oe in-plane applied field reveals a cusp at 177 K (2 K below the paramagnetic transition of dysprosium) and a significant increase at about 80 K. This is characteristic of a ferromagnetic cooperative phenomena inside the layers. Contrary to some observations<sup>8</sup> the onset of the ferromagnetic order inside the dysprosium layers is not enhanced by erbium. It is interesting to note that the antiferromagnetic intensity increases smoothly as the temperature decreases without any singularities when

crossing the successive magnetic transitions of erbium.

In conclusion, the Dy/Er superlattice system is unique in exhibiting long-range coupling of the dysprosium spins through an interlayer, which is itself a strongly magnetic element, but without inducing spin ordering in this erbium interlayer. The erbium spins ostensibly retain paramagnetic order. In addition an antiferromagnetic interlayer coupling is observed at low temperatures similar to that found recently in superlattices of dysprosium and the nonmagnetic element lutetium and explained by dipolar effects.<sup>3</sup> A number of interesting issues remain, in particular the origin of the coexistence of the antiferromagnetic and helical phases over a large temperature range, and details of the magnetism at the interface between layers of magnetic spins whose easy magnetization directions are perpendicular. These will be explored in future experiments.

This work was supported by NATO Grant No. 550-87. Laboratoire de Métallurgie Physique et Sciences des Matériaux is Unité de Recherche Associée au CNRS No. 155.

<sup>1</sup>R. W. Erwin, J. J. Rhyne, M. B. Salamon, J. Borchers, S. Sinha, R. Du, J. E. Cunningham, and C. P. Flynn, *Phys. Rev. B* **35**, 6808 (1987).

<sup>2</sup>J. A. Borchers, M. B. Salamon, R. W. Erwin, J. J. Rhyne, R. Du, and C. P. Flynn, *Phys. Rev. B* **43**, 3123 (1991).

<sup>3</sup>R. S. Beach, J. A. Borchers, A. Matheny, R. W. Erwin, M. B. Salamon, B. Everitt, K. Pettit, J. J. Rhyne, and C. P. Flynn, *Phys. Rev. Lett.* **70**, 3502 (1993).

<sup>4</sup>J. J. Rhyne, *Handbook on the Physics and Chemistry of Rare Earths*, edited by K. A. Gschneider, Jr., and LeRoy Eyring (North-Holland, Amsterdam, 1988), Vol. 11, Chap. 76.

<sup>5</sup>*Magnetic Properties of Rare-Earth Metals*, edited by R. J. Elliot (Plenum, New York, 1972), pp. 91 and 134.

<sup>6</sup>W. C. Koehler, *J. Appl. Phys.* **36**, 1078 (1965).

<sup>7</sup>J. Kwo, M. Hong, and S. Nakahara, *Appl. Phys. Lett.* **49**, 319 (1986).

<sup>8</sup>R. C. F. Farrow, S. S. P. Parking, V. S. Speriosu, A. Bezing, and A. P. Segmüller, in *Growth, Characterization and Properties of Ultrathin Magnetic Films and Multilayers*, edited by B. T. Jonker, J. P. Heremans, and E. E. Marinero, MRS Symposium Proceedings No. 151 (Materials Research Society, Pittsburgh, 1989), p. 203.